Development of a Superconducting Claw-Pole Linear Test-Rig

Development of a Superconducting Claw-Pole Linear Test-Rig

Patryk Radyjowski[1] , Ozan Keysan[2], Joseph Burchell[1], Markus Mueller[1]

[1]Institute for Energy Systems, University of Edinburgh, EH9 3JL, UK
[2] Electrical and Electronics Engineering Department, Middle East Technical University, Ankara, Turkey

E-mail: keysan@metu.edu.tr

Abstract.

Superconducting generators can help to reduce the cost of energy for large offshore wind turbines, where the size and mass of the generator have a direct effect on the installation cost. However, existing superconducting generators are not as reliable as the alternative technologies. In this paper, a linear test prototype for a novel superconducting claw pole topology, which has a stationary superconducting coil that eliminates the cryocooler coupler will be presented. The issues related to mechanical, electromagnetic and thermal aspects of the of the prototype will be presented.

1. Introduction

Average size of offshore wind turbines is constantly increasing in an effort to reduce the installation and maintenance cost per MW. The aim of the industry is to manufacture 10 MW wind turbines; for this purpose various superconducting generator designs have been suggested [1, 2]. In previous studies, it has been proposed that superconducting generators have the potential to significantly reduce the tower head mass for 10 MW offshore wind turbines [3, 4, 5, 6, 7, 8]. Superconducting generators have higher torque densities compared to conventional generators thanks to the increased specific magnetic loading, which is a result of high MMF generated by the superconducting field windings. A mass comparison between HTS and conventional generators are presented in [9]. It is showed that 10 MW, 10 rpm HTS machines weight around 100–150 tonnes compared to 300–350 tonnes of direct-drive permanent-magnet generators.

However, affordability is always a primary concern for the superconducting power applications [10] and the success of the superconducting technologies in renewable energy market is directly related to the cost vs. performance values compared to existing mature technologies [11]. It should be noted that it is not only the initial cost of the generator that should be taken into account, but also the maintenance and the repair cost, which can be significant in harsh offshore environment. However, the issue of reliability of superconducting machines is usually ignored in most of the proposed designs. Another neglected topic in superconducting machines is the structural mass, which is expected to be much higher than conventional machines due to increased magnetic attraction forces. In order to address these two issues, a new topology has been proposed in [9], in which a modular claw-pole topology and a stationary superconducting field winding are used.

The advantages of the proposed topology compared to other superconducting machine designs can be listed as:

- The machine has a stationary superconducting field winding, which means: no cryocoupler, no brushes or brushless exciters, no vibrational or rotational forces acting on the SC coil. Thus the reliability of the machine is improved.
- The machine uses significantly less superconducting coil due to iron-cored structure and loop-shaped field winding. It is shown in [9] that just 15 km of MgB2 wire is required for a 10 MW machine.
- The machine has two armature windings that can be operated independently. Thus, the modularity is increased.

However, the proposed topology has a few drawbacks as well:

- Although, the proposed design is still lighter than direct-drive permanent-magnet generators, due to iron-cored structure of the proposed topology, the cost reduction is not as significant as the other superconducting machine types.
- The proposed machine is expected to have a low power-factor, which is a drawback of transverse-flux machines in general.

In this paper, details of a linear prototype that has the same claw-pole topology presented in [9] will be presented. The main aim is to address practical issues in the structural and thermal design that can create problem in the full-scale rotational machine. Although, the linear generator is produced as a scaled-down version of a rotational machine, it is also possible to apply the linear topology as a linear superconducting generator (e.g. for wave energy converters).

2. Linear Prototype

A linear machine prototype is designed and manufactured to prove operation of the superconducting claw pole machine topology. The main idea is to generate the magnetic field using a stationary superconducting field winding, and to obtain varying magnetic field in the armature coils by modulating the field flux and using claw-pole shaped iron cored rotor. The main sections of the linear prototype are presented in Figure 1a and 1b. The translator, which consists of modular claw poles, is placed between the armature core and the field core, which supports the stationary superconducting field winding. During operation, the magnetic field created by the superconducting coil is diverted to the armature core and to the concentrated armature coils. The translator, field core and armature core are manufactured using electrical steel laminations.

The linear machine is modelled with 3D electromagnetic FEA software. Figure 1c and 1d shows the flux density distribution and flux vectors in the machine when the field core is excited. It can be seen that the claw poles are heavily saturated (up to 1.84T) and link the field core with the armature core. Since the magnetization direction of each claw pole does not change with the position of the translator, the core loss in the translator is negligible .

3. Mechanical Aspects

In most electrical machines, there is a magnetic attraction force between rotor and stator, which tries to close the air-gap clearance. The mechanical structure of the rotor must be stiff enough to withstand this pressure, which can be calculated using the normal component of the Maxwell Stress:

$$P = \frac{B_{ag}^2}{2\mu_0} \quad \mathrm{N/m^2} \tag{1}$$

where B_{ag} is the flux density magnitude in the air-gap, and μ_0 is the permeability of air. The pressure is around 200 kN/m^2 for a typical electrical machine where the air gap flux density is around 0.7 T. However, this pressure increases to 1600 kN/m^2, if the flux density is raised upto to 2 T, which can be achieved in a superconducting machine.

Due to increase in these attraction forces, the structural loads will increase in a superconducting machine, which will require a significant amount of added structural mass in order to maintain the air-gap clearance. One may argue that, in rotational machines the forces acting on the rotor are cancelled due to the rotational symmetry,

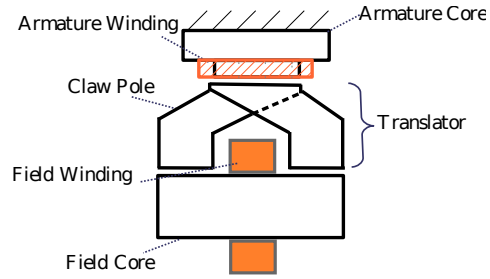

(a) Schematic of the linear claw pole machine (front view).

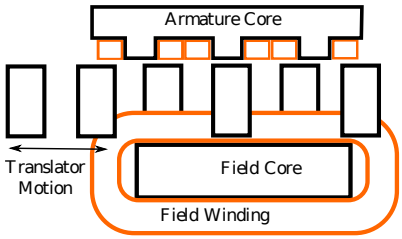

(b) Side view.

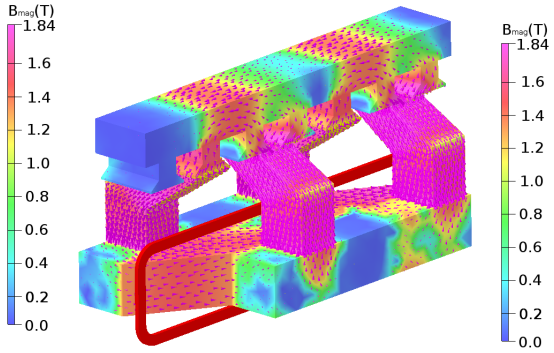

(c) Flux density distribution and flux vectors in the linear prototype

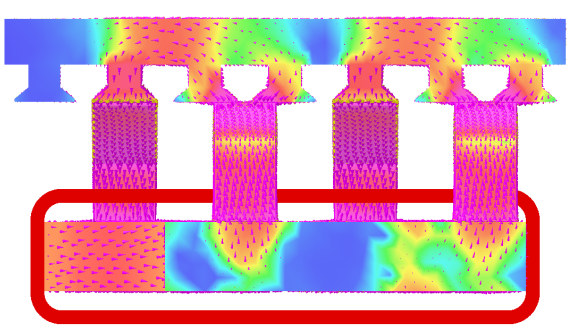

(d) Flux density vectors (side view).

Figure 1: Linear claw-pole superconducting machine design.

however, it may not be the case due to eccentricity or any other non-symmetries due to machine topology.

The total mass of the translator (see Figure 1) is approximately 15 kg, which imposes a gravitational force of 150 N in the -Y direction (downwards). The translator of the linear prototype is supported by four linear bearings and can be moved freely. Magnetic attraction forces are existent on the both sides of the claw-pole (i.e. between the armature core and the field core). However, forces on the lower gap are higher due to concentrated flux density. Thus, the orientation of the translator is turned upside-down to cancel the gravitational force with magnetic attraction forces. When the machine is excited in this configuration, the Maxwell stress acting on the translator is 305 N in the +Y direction (upwards). Thus, the net force acting on the translator is changing between -150 N and +155 N in Y direction and the forces are kept within limits for the linear bearings.

4. Superconducting Coil & Support Structure

There are a few suitable materials for superconducting generators such as: YBCO, MgB2, NbTi and BSCCO. Properties and cost of these materials are compared in [10]. In the linear prototype, superconducting coils that are used previously in the Hydrogenie project (an EU-funded project on development of a 1.7 MW superconducting

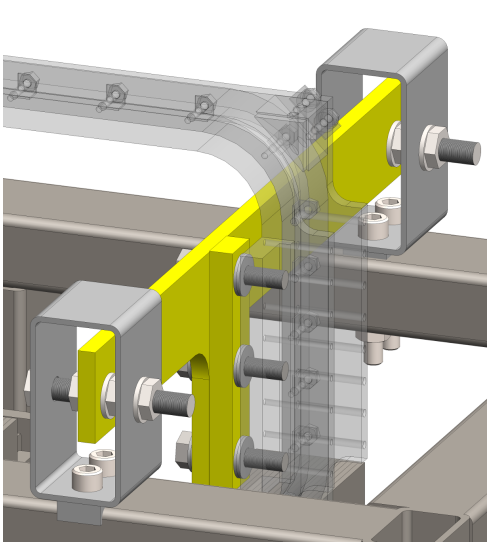

(a) CAD model of the coil support

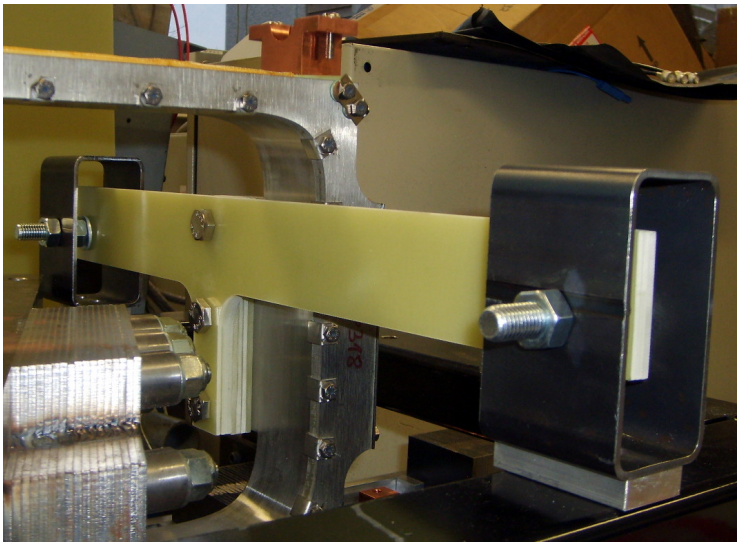

(b) Photo of the fibreglass support.

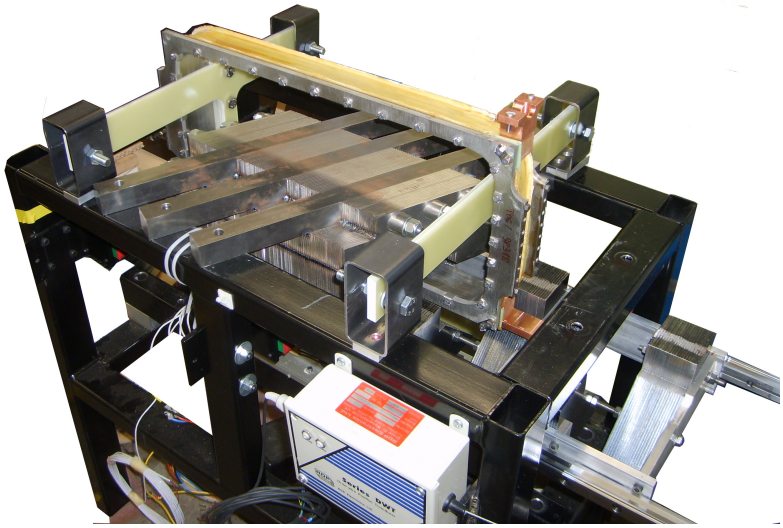

(c) Photo of the linear prototype

Figure 2: Support structure for the superconducting field winding.

hydroelectric power generator [12]) are used. The winding, which employs Bi-2223 tape conductor, has 200 turns, 50 cm length and 25 cm width. The superconducting tape is rated at 145 A (self-field at 77 K).

The superconducting coil is fixed to the main frame using a stack of 1/8" thick cryogenic grade fibreglass cut-outs as shown in Figure 2. The NP500CR(EU)/G10CR(US) fibreglass material has been chosen because of its certified ability to withstand temperatures down to 4 K while providing a satisfactory balance between structural strength and thermal insulation capabilities. This material has been proven in many structural applications in cryogenic systems where low thermal conductivity was of importance [13]. The sheets are made of a special halogen-free

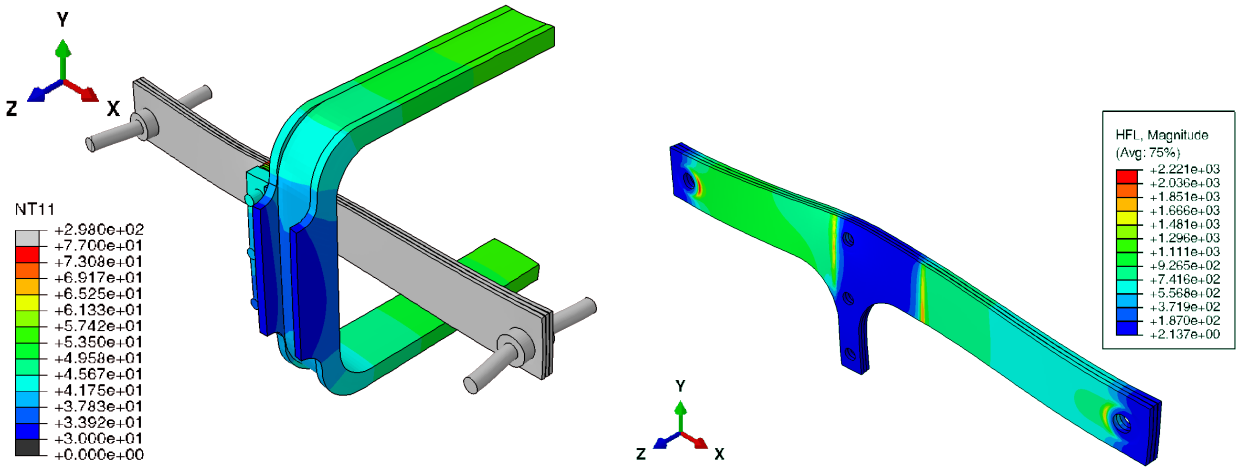

(a) Temperature Distribution. (b) Heat Flux.

Figure 3: Thermal FEM analysis of the coil assembly.

resin, which retains its properties at very low temperatures and prone to cracking due to embrittlement.

Another issue is the different thermal expansion constants of G10-CR and A304 steel. If uncompensated, it will lead to loosening of the fastener upon the cool-down and result in a faulty joint. Bellevue (spring) washers positioned on both sides of fibreglass stack to eliminate this problem.

5. Thermal Aspects

Thermal FEA simulations are performed on the support structure to calculate heat flux, temperature distribution and Van Misses stresses due to thermal contraction. The temperature distribution in the superconducting coil is presented in Figure 3a. The shear stress (Y direction) in the support structure is found to be 77 kPa and the bending stress (Z direction) is 66 MPa, which gives a safety factor of 6. The simplified Van Misses stress is found as 82.3 MPa (See Figure 3a), which gives a safety factor of 4.8. There are regions of significant stress concentrations around the mounting holes, which are due to a small contact area of compressed spring washers. This can be avoided by using the secondary flat washer, which will spread the compression force on greater area. Another outcome of the FEM simulations is the heat flux distribution as presented in Figure 3b. The average values for heat flux are: $800\frac{W}{m^2}$ for the short arm (0.6 W total), and $1000\frac{W}{m^2}$ for the long arm (0.76 W total).

The main mode of heat transfer through the support arm is the conduction in fibreglass, which can be calculated as 1.37 W using the FEA simulations. The vast thermal gradient necessary for superconducting systems requires the use of Multi Layer Insulation (MLI) in order to minimize the cooling cost. The design has a 10 mm spacing between cold and warm parts, which will be filled with MLI blankets. Based on the MLI performance values supplied in [14] and with a conservative working pressure of 1 Pa,

the expected radiation heat flux through the 10 mm MLI blanket can be calculated as $5.4\,\mathrm{W/m^2}$:

$$Q''_{in} = \frac{k_{MLI}\Delta T}{L_{MLI}} = \frac{0.0002 \cdot (300 - 30)}{0.01} \approx 5.4\,\mathrm{W/m^2} \tag{2}$$

Finally, the full system simulation allows to predict the temperature distribution, which has been presented in Figure 3a. Based on the worst case scenario with all heat loads doubled (MLI thickness is halved to 5 mm, where the heat load of the current leads is 4 W) the maximum temperature of the coil is below 57 K, which satisfies the design specifications.

6. Current Leads

The current leads have to supply 60 A from a warm environment into the HTS coil. The total heat loss in the current leads is the resultant of material conduction and ohmic heating. In large scale applications it is possible to use a hybrid resistive-superconducting current leads. However, in this case a simple resistive copper connection with a thermal intercept and a thick copper heat sink should be utilized to minimize the heat loss into the HTS coil.

The built-in power connectors are extended by screwing copper parts, which are used to clamp into cooling pipes with a thin lining of Kapton foil to provide an electrical insulation. Kapton foil provides high electric insulation properties (up to 7.7 kV) at a very small thickness (0.0254 mm). The completed attachment system is presented in Figure 4a.

7. Actuator & Crysotat Integration

The whole linear machine is planned to be placed into a big vacuum chamber (see Figure 4b), which has a diameter of 2.4 m and height of 1.2 m, as shown in Figure 4c with the vacuum pumps and the helium cryocooler. Since, the entire machine is placed in vacuum, a linear actuator is required to move the translator during tests. A vacuum graded stepper motor and a lead-screw assembly(see Figure 4a) are used for this purpose. The chosen motor is a Phytron VSS42.200, which generates 0.09 Nm torque at 1.2 A. The instruments are interfaced through a Subminiature-D 25-pin connection embedded in a LF-63 flange.

Due to lack of thermal convection in vacuum the joule heating in the copper supply cable becomes a significant issue. Furthermore, commonly used insulation materials such as thermoplastics and poly-carbonates are not suitable for the use in vacuum due to degassing issues. Although, Teflon based materials are usually used in vacuum applications, a self-manufactured Kapton insulation of bare copper wire is preferred in the current project. Two parallel copper wires each carrying 30 A are chosen. The heat load and temperature distribution along the 2 m cable, with a cold end fixed at 30 K, are presented in Figure 5. Residual-resistivity ratio (RRR) of the copper is

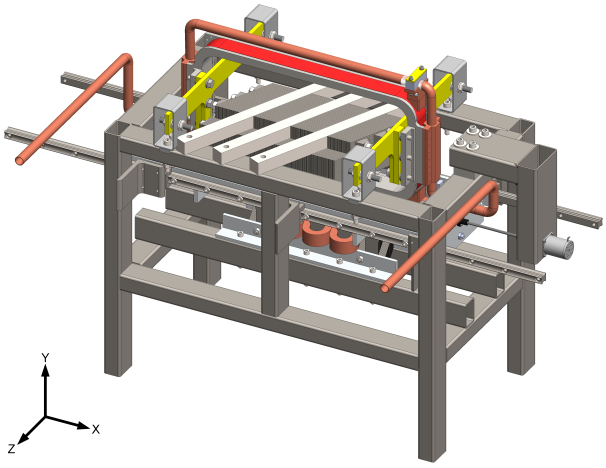

(a) Linear prototype with HTS coil and the cooling pipes

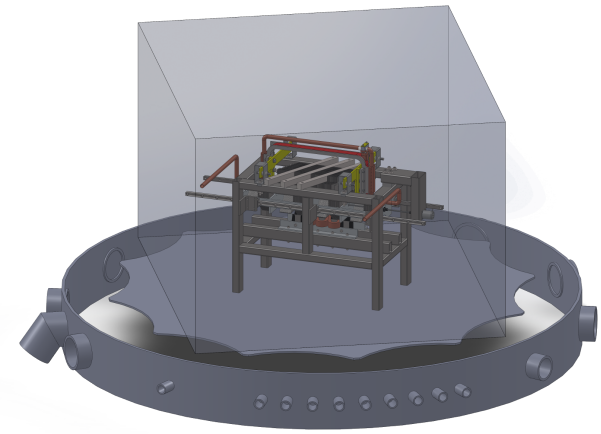

(b) Linear prototype positioned in the vacuum chamber (Diameter of the cryostat is 2.4 m, height is 1.2 m).

(c) Vacuum chamber with helium cryocoolers [12].

Figure 4: Placement of linear prototype in the vacuum chamber.

chosen as 200. The analytical model accounts for the ohmic heating together with conduction and radiation heat transfer only, as there is no convection heat loss in the vacuum. The calculations show that the temperature of the 2.6 mm supply cable in the vacuum chamber can increase up to 365 K, but even in this case the thermal load to the cryocooler is lower than the 4.1 mm cable.

8. Conclusion

This paper presented the initial prototype of a claw-pole superconducting machine topology. The biggest advantage of the prototype is having a stationary superconducting field winding, which simplifies the cooling system and eliminates the mechanical issues associated with a rotating superconducting field winding.

However, it is clear that the electromagnetic design of an HTS machine cannot be finalized without addressing issues of thermal and mechanical problems associated

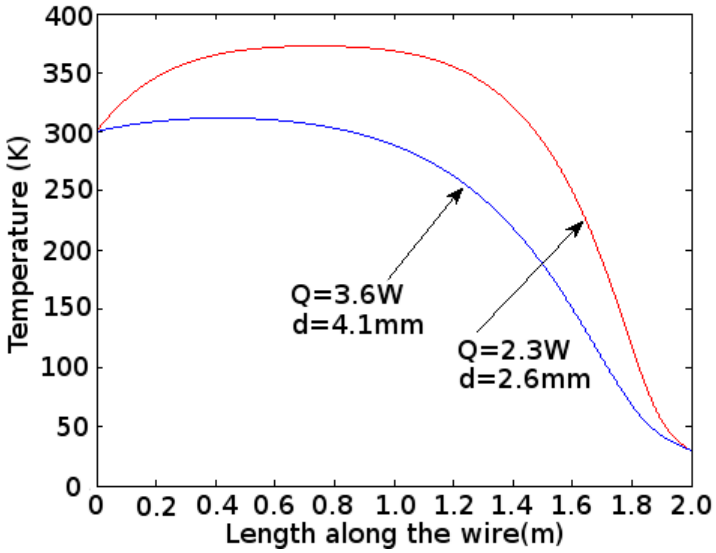

Figure 5: Heat load and distribution of the temperature along the current feeding cable.

with the superconducting coil. Therefore, a small prototype is built to solve these issues as early as possible by addressing the possible problems in manufacturing and structural design. In particular, thermal and mechanical design of the superconducting coil support structure is investigated. The prototype is planned to be tested in a big vacuum chamber, under different field excitation and speeds in near future.

References

[1] A. B. Abrahamsen, N. Mijatovic, E. Seiler, T. Zirngibl, C. Træ holt, P. B. Norgå rd, N. F. Pedersen, N. H. Andersen, and J. Ostergå rd, "Superconducting wind turbine generators," *Superconductor Science and Technology*, vol. 23, no. 3, p. 034019, Mar. 2010. [Online]. Available: http://iopscience.iop.org/0953-2048/23/3/034019/

[2] B. Maples, M. Hand, and W. Musial, "Comparative Assessment of Direct Drive High Temperature Superconducting Generators in Multi-Megawatt Class Wind Turbines," National Renewable Energy Laboratory (NREL), Golden, CO., Tech. Rep. October, 2010. [Online]. Available: http://www.osti.gov/bridge/product.biblio.jsp?osti_id=991560

[3] G. Snitchler, B. Gamble, C. King, and P. Winn, "10 MW Class Superconductor Wind Turbine Generators," *IEEE Transactions on Applied Superconductivity*, vol. 21, no. 3, pp. 1089–1092, Jun. 2011. [Online]. Available: http://ieeexplore.ieee.org/lpdocs/epic03/wrapper.htm?arnumber=5699957

[4] P. J. Masson, "Wind Turbine Generators: Beyond the 10MW Frontier," in *Symposium on Superconducting Devices for Wind Energy Systems*, 2011, pp. 1–8.

[5] F. Fair, W. Stautner, M. Douglass, R. Rajput-Ghoshal, M. Moscinski, P. Riley, D. Wagner, J. Kim, S. Hou, F. Lopez, K. Haran, J. Bray, T. Laskaris, J. Rochford, R. Duckworth, D. Wagner, J. Kim, S. Hou, F. Lopez, K. Haran, J. Bray, T. Laskaris, J. Rochford, and R. Duckworth, "Next Generation Drive Train - Superconductivity for Large-Scale Wind Turbines," in *Applied Superconductivity Conference*, no. 22, Portland, Oregon, 2012, pp. 1–29. [Online]. Available: http://www.ewh.ieee.org/tc/csc/europe/newsforum/pdf/STP307.pdf

[6] H. Sung, G. Kim, K. Kim, S. Jung, M. Park, I. Yu, Y. Kim, H. Lee, and A. Kim, "Practical

Design of a 10 MW Superconducting Wind Power Generator Considering Weight Issue," *IEEE Transactions on Applied Superconductivity*, vol. 23, no. 3, p. 5201805, Jun. 2013. [Online]. Available: http://ieeexplore.ieee.org/lpdocs/epic03/wrapper.htm?arnumber=6449292

[7] S. Sanz, T. Arlaban, R. Manzanas, M. Tropeano, R. Funke, P. Kováč, Y. Yang, H. Neumann, and B. Mondesert, "Superconducting light generator for large offshore wind turbines," *Journal of Physics: Conference Series*, vol. 507, no. 3, p. 032040, May 2014. [Online]. Available: http://stacks.iop.org/1742-6596/507/i=3/a=032040?key=crossref.4a6e5b094a41e85ba8429050a363ff55

[8] S. S. Kalsi, "Superconducting Wind Turbine Generator Employing MgB2 Windings Both on Rotor and Stator," *IEEE Transactions on Applied Superconductivity*, vol. 24, no. 1, pp. 47–53, Feb. 2014. [Online]. Available: http://ieeexplore.ieee.org/lpdocs/epic03/wrapper.htm?arnumber=6670049

[9] O. Keysan and M. Mueller, "A Modular and Cost-Effective Superconducting Generator Design for Offshore Wind Turbines," *Superconductor Science and Technology*, vol. 28, no. 3, p. 34004, 2015. [Online]. Available: http://dx.doi.org/10.1088/0953-2048/28/3/034004

[10] N. Martucciello, F. Giubileo, G. Grimaldi, and V. Corato, "Introduction to the focus on superconductivity for energy," *Superconductor Science and Technology*, vol. 28, no. 7, p. 070201, 2015. [Online]. Available: http://stacks.iop.org/0953-2048/28/i=7/a=070201?key=crossref.606087f2eb5e273bfbfe122432876c52

[11] a. M. Campbell, "Superconducting and conventional machines," *Superconductor Science and Technology*, vol. 27, no. 12, p. 124012, 2014. [Online]. Available: http://stacks.iop.org/0953-2048/27/i=12/a=124012?key=crossref.eabd908f703511ad50f68d1d7055d4a1

[12] R. Fair, C. Lewis, J. Eugene, and M. Ingles, "Development of an HTS hydroelectric power generator for the hirschaid power station," *Journal of Physics: Conference Series*, vol. 234, no. 3, p. 032008, Jun. 2010. [Online]. Available: http://stacks.iop.org/1742-6596/234/i=3/a=032008?key=crossref.31e5bf4ab2e26dd131adb7d0fcc02f6b

[13] R. P. Reed and M. Goldat, "Cryogenic composite supports : a review of strap and strut properties," vol. 37, no. 5, pp. 233–250, 1997.

[14] J. E. Fesmire, S. Augustynowicz, and C. Darve, "Performance characterization of perforated multilayer insulation blankets," in *19th International Cryogenic Engineering Conference*, G. G. Baguer and N. P.Seyfert, Eds. Grenoble, France: Narosa Publishing House, 2002, pp. 843–846.